Categorical Symmetries in Spin Models with Atom Arrays

Alison Warman,[1,*] Fan Yang,[2,3,†] Apoorv Tiwari,[4] Hannes Pichler,[2,3] and Sakura Schäfer-Nameki[1]
[1]Mathematical Institute, University of Oxford, Woodstock Road, Oxford OX2 6GG, United Kingdom
[2]Institute for Theoretical Physics, University of Innsbruck, Innsbruck 6020, Austria
[3]Institute for Quantum Optics and Quantum Information of the Austrian Academy of Sciences, Innsbruck 6020, Austria
[4]Center for Quantum Mathematics at IMADA, Southern Denmark University, Campusvej 55, 5230 Odense, Denmark

(Received 19 February 2025; revised 1 July 2025; accepted 25 August 2025; published 13 November 2025)

Categorical symmetries have recently been shown to generalize the classification of phases of matter, significantly broadening the traditional Landau paradigm. To test these predictions, we propose a simple spin chain model that encompasses all gapped phases and second-order phase transitions governed by the categorical symmetry $\mathsf{Rep}(D_8)$. This model not only captures the essential features of noninvertible phases but is also straightforward enough to enable practical realization. Specifically, we outline an implementation using neutral atoms trapped in optical tweezer arrays. Employing a dual-species setup and Rydberg blockade, we propose a digital simulation approach that can efficiently implement the many-body evolution in several nontrivial quantum phases.

DOI: 10.1103/249m-m8wq

Introduction—Symmetries are fundamental in studying and constraining phases of matter, and were traditionally limited to groups. This framework underpins a wide range of theoretical physics, from quantum mechanics and condensed matter to quantum field theory. However, recent developments have revealed that symmetries in any dimension are far more general and form so-called (higher) fusion categories, characterized by the key property that not every symmetry transformation has an inverse. In recent years, these categorical or noninvertible symmetries have been recognized as ubiquitous, with far-reaching implications, including a categorical extension of the Landau paradigm of phases, new constraints on standard model physics, and advances in formal quantum field theory (for reviews, see Refs. [1,2]). Our aim is to establish a framework that allows direct testing of certain predictions from categorical symmetries in quantum simulators realizing spin chains.

Phases with categorical symmetries—In $(1+1)$d the most general (finite and internal) symmetry structure is a fusion category, whose generators $\{a, b, c, \ldots\}$ satisfy the composition $\otimes$ rule $a \otimes b = \sum_c N_{ab}^c c$, where N_{ab}^c are non-negative integers, which in general is not an invertible operation. Phases with these symmetries are described by a categorical extension of the Landau paradigm, and feature novel symmetry-breaking patterns and new symmetry-protected critical models. A systematic characterization of all gapped and gapless phases was recently proposed [3–10] using the so-called symmetry topological field theory [11–16]. This computes all symmetric gapped phases, including the order parameters, ground states, and the action of the categorical symmetry on the phases. The theory furthermore predicts new second-order phase transitions, which are gapless phases with categorical symmetries.

Lattice models and cold atom implementation—This Letter aims to explore these phenomena through simple spin chains that realize categorical phases, while also proposing an experimental protocol to probe them. This is particularly interesting for systems that may have phase transitions that are hard to study numerically—examples are precisely categorical symmetries with, e.g., the Haagerup symmetry being one of the most notorious (for recent progress see Refs. [18–20]). Lattice models with a categorical symmetry can be systematically constructed from the anyon chain [21], which generically results in a constrained Hilbert space [22–29]. This approach allows a systematic construction of commuting projector Hamiltonians for all gapped phases and second-order phase transitions of a categorical symmetry [29].

In this Letter, we present a benchmark spin chain that demonstrates all the characteristic features of phases with noninvertible symmetries. Inspired by this general approach, the model has the distinctive advantage of being realized in an unconstrained tensor product Hilbert space based on qubits, as illustrated in Fig. 1(a). Its Hamiltonians take the following schematic form:

*Contact author: warman@maths.ox.ac.uk
†Contact author: F.Yang@uibk.ac.at

Published by the American Physical Society under the terms of the Creative Commons Attribution 4.0 International license. Further distribution of this work must maintain attribution to the author(s) and the published article's title, journal citation, and DOI.

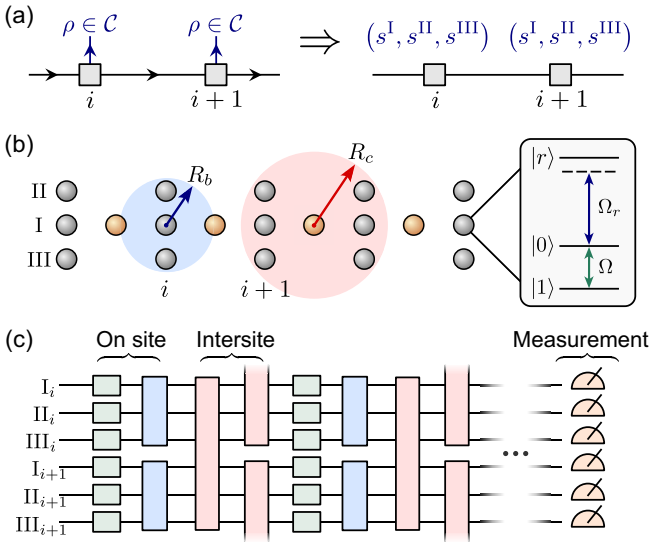


FIG. 1. (a) The anyon chain for a categorical symmetry (left) is used to construct lattice models, generically on a constrained Hilbert space. Here, we realize this on a spin chain, realized on an unconstrained three-qubit tensor product Hilbert space (right). (b) Lattice configuration and atomic level diagram used in our proposal for realizing the spin chain in (a) with categorical symmetry. The silver and the golden circles represent the data and the ancillary atomic qubits, respectively. (c) Trotterization scheme of the quantum circuit for simulating the many-body dynamics. On-site and intersite terms can be realized by only driving data atoms or ancillary atoms, respectively.

$$H = \sum_i V_{i,i+1} + \sum_i P_i, \tag{1}$$

where P_i denotes a projector acting on a few spins at a given site i, while $V_{i,i+1}$ is the interaction between neighboring sites i and $i+1$. This system not only captures all the key noninvertible features but is also well-suited for experimental implementation. For the latter, we focus on implementations with Rydberg-atom arrays, which have emerged as promising platforms for quantum simulation of spin models [30–33]. These systems have already been used to experimentally probe quantum phase transitions breaking conventional discrete [34–37] and continuous [38] group symmetries, as well as topologically ordered phases [39]. Here, we discuss how these systems can be used to experimentally probe phases with noninvertible symmetries and the transitions between them. Specifically, our proposal is based on a digital evolution that can be induced by two driving lasers in a dual-species Rydberg atom array [40,41], as shown in Fig. 1(b).

Benchmark model: $\mathsf{Rep}(D_8)$ *categorical symmetry*—The benchmark symmetry is $\mathsf{Rep}(D_8)$, i.e., the representations of the finite group $D_8 \coloneqq (\mathbb{Z}_2^a \times \mathbb{Z}_2^b) \rtimes \mathbb{Z}_2^c$ of symmetries of the square (rotations and reflections). The generators are the irreducible representations (irreps),

$$\text{Generators of } \mathsf{Rep}(D_8)\text{: } 1, 1_c, 1_a, 1_{ca}, E, \tag{2}$$

with $\dim(1_k) = 1$, $\dim(E) = 2$, and their composition is the tensor product of irreps with $k = a, c, ca$,

$$\begin{aligned} &1_a \otimes 1_c = 1_c \otimes 1_a = 1_{ca}, \qquad 1_k \otimes 1_k = 1, \\ &E \otimes 1_k = 1_k \otimes E = E, \\ &E \otimes E = 1 \oplus 1_a \oplus 1_c \oplus 1_{ca}, \end{aligned} \tag{3}$$

the last line being a noninvertible composition rule. Using recent advancements in the representation theory of categorical symmetries, we can now demonstrate the full scope of the categorical Landau paradigm in action. This includes a comprehensive characterization of gapped phases and phase transitions [10]. Lattice models for a subset of these phases have recently been realized using a complementary approach based on the cluster state [42–44]. In this Letter, we show that all phases can be captured within a straightforward tensor product Hilbert space constructed from qubits.

The benchmark model provides a (1) derivation of all gapped and gapless phases governed by $\mathsf{Rep}(D_8)$, exhibiting the key features of categorical symmetries; (2) realization in simple spin models, with few-body interactions; and (3) realistic near future implementation of the spin model in Rydberg atom arrays. Our Letter furthermore opens up avenues for exploring dynamical questions, such as those related to quantum quenches, for which accurate and efficient analytic or numerical tools are currently lacking.

Gapped phases for $\mathsf{Rep}(D_8)$—There are 11 distinct gapped phases for $\mathsf{Rep}(D_8)$, which can be labeled by (F, β), where F is a representative of a conjugacy class of subgroups of D_8 and a cocycle $\beta \in H^2[F, U(1)]$ [10,17].

On general grounds [29], the gapped phases for this symmetry can be realized on a lattice model, where the states are labeled by group elements $\mathsf{g}, \mathsf{h} \in D_8$ and operators acting as

$$L^{\mathsf{g}}|\mathsf{h}\rangle = |\mathsf{gh}\rangle, \qquad R^{\mathsf{g}}|\mathsf{h}\rangle = |\mathsf{hg}\rangle. \tag{4}$$

The commuting projector Hamiltonians for the gapped phases take the general form (1), and are given by [45]

$$H_{(F,\beta)} = -\frac{1}{|F|}\sum_i \sum_{\mathsf{f}\in F} (R_\beta^{\mathsf{f}^{-1}})_i (L_\beta^{\mathsf{f}})_{i+1} - \sum_i P_i^{(F)}. \tag{5}$$

Here, $P^{(F)}$ is a projector onto the F subgroup of D_8 [46]. For each $\mathsf{Rep}(D_8)$ irrep Γ, and $l, m \in \{1, \ldots, \dim(\Gamma)\}$, we introduce a (diagonal) operator $Z_\Gamma^{l,m}$ that acts as [47]

$$Z_\Gamma^{l,m}|\mathsf{g}\rangle = \mathcal{D}_\Gamma^{l,m}(\mathsf{g})|\mathsf{g}\rangle, \tag{6}$$

where $\mathcal{D}_\Gamma(\mathsf{g})$ represents g in the irrep Γ.

The simplification, which is key to the potential realization in future experiments, is the identification of the state space with that of three qubits,

$$|s^{\mathrm{I}}s^{\mathrm{II}}s^{\mathrm{III}}\rangle, \qquad s^{\alpha}\in\{0,1\}, \tag{7}$$

via the mapping

$$\begin{aligned}
&|1\rangle\mapsto|000\rangle, \quad |a\rangle\mapsto|010\rangle, \quad |b\rangle\mapsto|001\rangle,\\
&|c\rangle\mapsto|100\rangle, \quad |ca\rangle\mapsto|101\rangle, \quad |cb\rangle\mapsto|110\rangle,\\
&|ab\rangle\mapsto|011\rangle, \quad |cab\rangle\mapsto|111\rangle.
\end{aligned} \tag{8}$$

The Hamiltonians for each phase can thus be written in terms of Pauli operators X_i^{α} and Z_i^{α} acting on qubit $\alpha=\mathrm{I},\mathrm{II},\mathrm{III}$ at site i,

$$\begin{aligned}
L^a&=X^{\mathrm{II}}, \quad & R^a&=Q^{\mathrm{I},+}X^{\mathrm{II}}+Q^{\mathrm{I},-}X^{\mathrm{III}},\\
L^b&=X^{\mathrm{III}}, \quad & R^b&=Q^{\mathrm{I},-}X^{\mathrm{II}}+Q^{\mathrm{I},+}X^{\mathrm{III}},\\
L^c&=X^{\mathrm{I}}(\mathrm{Swap})^{\mathrm{II,III}}, \quad & R^c&=X^{\mathrm{I}},
\end{aligned} \tag{9}$$

where $Q^{\alpha,\pm}=\frac{1}{2}(1\pm Z^{\alpha})$ and $(\mathrm{Swap})^{\mathrm{II,III}}$ swaps II and III. The symmetry operators $\mathcal{S}_{\Gamma}$ for each irrep Γ are

$$\begin{aligned}
&\mathcal{S}_{1_a}=\prod_i Z_i^{\mathrm{I}}, \quad \mathcal{S}_{1_c}=\prod_i Z_i^{\mathrm{II}}Z_i^{\mathrm{III}}, \quad \mathcal{S}_{1_{ca}}=\prod_i Z_i^{\mathrm{I}}Z_i^{\mathrm{II}}Z_i^{\mathrm{III}},\\
&\mathcal{S}_E=Z^{1,1}_{E,\mathrm{prod}}+Z^{2,2}_{E,\mathrm{prod}},
\end{aligned} \tag{10}$$

where for the two dimensional irrep E, with matrix representation $\mathcal{D}_E(a)=Y$, $\mathcal{D}_E(b)=-Y$, $\mathcal{D}_E(c)=X$, $Z_{E,\mathrm{prod}}=\prod_i(Z_E)_i$ is the product of the matrix

$$\begin{aligned}
Z_E^{1,1}&=Q^{1_{ca},+}(S^{\mathrm{I}})^{\dagger}Z^{\mathrm{III}},\\
Z_E^{1,2}&=Q^{1_{ca},-}(S^{\mathrm{II}})^{\dagger}S^{\mathrm{III}}(CZ)^{\mathrm{II,III}},\\
Z_E^{2,1}&=Q^{1_{ca},-}S^{\mathrm{II}}(S^{\mathrm{III}})^{\dagger}(CZ)^{\mathrm{II,III}},\\
Z_E^{2,2}&=Q^{1_{ca},+}S^{\mathrm{I}}Z^{\mathrm{III}},
\end{aligned} \tag{11}$$

on all the lattice sites, with $Q^{1_{ca},\pm}=\frac{1}{2}(\mathbb{I}\pm Z^{\mathrm{I}}Z^{\mathrm{II}}Z^{\mathrm{III}})$, $S=\mathrm{diag}(1,i)$, and $CZ=\mathrm{diag}(1,1,1,-1)$.

The symmetry operators $\mathcal{S}_{\Gamma}$ act on states as $\mathcal{S}_{\Gamma}|\Psi_{\mathsf{g}}\rangle=\mathrm{Tr}[\mathcal{D}_{\Gamma}(\mathsf{g})]|\Psi_{\mathsf{g}}\rangle$, where g is the "holonomy" of the state, i.e., the product of all the group elements on the lattice sites. The diagonal operators $\mathcal{S}_{\Gamma}$ commute with $H_{(F,\beta)}$ since $P^{(F)}$ is also diagonal and since $\mathcal{D}_{\Gamma}(\mathsf{f}^{-1})\mathcal{D}_{\Gamma}(\mathsf{f})=\mathbb{I}$; hence the Hamiltonians (5) are $\mathsf{Rep}(D_8)$-symmetric. Their ground states are linear combinations of $|\Psi_{[f]}\rangle$ for $f\in F$, from which we can compute the $\mathsf{Rep}(D_8)$ symmetry action, as detailed in Supplemental Material (SM) [49].

The gapped phases, with their Hamiltonians, are summarized in the End Matter, Table I. They are either symmetry protected topological (SPT) or spontaneous symmetry breaking (SSB) phases for particular subsymmetries of $\mathsf{Rep}(D_8)$. For the first five phases, one can first minimize the projector $-(\mathbb{I}+Z^{\mathrm{I}})_i/2$ by setting $s^{\mathrm{I}}=0$ on all sites. On this subspace, $\mathcal{S}_E$ reduces to $\mathcal{S}_E\simeq\prod_i Z_i^{\mathrm{II}}+\prod_i Z_i^{\mathrm{III}}$, and the simplified Hamiltonians in Table I (bold terms) involve up to four-body interactions between sites $\{\mathrm{II}_i,\mathrm{III}_i,\mathrm{II}_{i+1},\mathrm{III}_{i+1}\}$. As we will show below, this simplification can reduce the complexity of our experimental scheme.

Phase transitions—One of the most recent advances is the systematic study of second-order phase transitions between two gapped phases with categorical symmetries, facilitated by the symmetry topological field theory framework [7,8,10,29]. In simple spin-chain models, we can furthermore analyze the interpolation between two gapped phases with Hamiltonians $H_{(l)}$ or $H_{(m)}$ respectively,

$$H_{(l,m)}(\lambda)=\lambda H_{(l)}+(1-\lambda)H_{(m)}, \tag{12}$$

where for some value between 0 and 1 we have the gapless Hamiltonian for the critical point describing the second-order phase transition between the two gapped phases. From the general continuum analysis in [10] one can determine furthermore the conformal field theories (CFTs) that describe these transitions, which we corroborate from by a spin-chain analysis in SM [49], where we show that the transitions can be realized within this simple framework.

Hardware-efficient simulation scheme—We now turn to a potential implementation of these spin models with Rydberg atom arrays. While these systems often realize spin models in an analog way [36,37,63–66], here we propose a digital approach [67–70] that is versatile enough to accommodate the first five phases in Table I, and potentially can be extended to the remaining ones.

The configuration of the atom array is illustrated in Fig. 1(b): for each lattice site i, a group of three atoms is aligned perpendicular to the direction of the chain, representing spins $\{\mathrm{I}_i,\mathrm{II}_i,\mathrm{III}_i\}$ as in Eq. (7). These atomic data qubits are encoded by two long-living hyperfine ground states $|1\rangle$ (spin-down) and $|0\rangle$ (spin-up). The latter state can be further coupled to a Rydberg state $|r\rangle$ for inducing interactions between qubits via the Rydberg blockade mechanism [71]. We assume that certain subsets of the atoms on each site can be addressed by the Rydberg laser, e.g., by shifting the other atoms out of resonance using a few distinct tweezer patterns [72]. In addition, an ancillary atom of a different species is placed between two neighboring sites i and $i+1$ [see Fig. 1(b)]. These ancillary atoms have an analogous level scheme as our data atoms, but can be driven independently from them. Moreover, this dual-species setup supports an asymmetric Rydberg blockade, in which the intra- and the interspecies blockade radius (R_b and R_c) can be independently tuned, e.g., via Förster resonance [41]. Here, we choose $R_c>R_b$ such that each data qubit can only be blockaded by its on-site nearest

neighbors (I_i and II_i; I_i and III_i) or two closest ancillary qubits [see Fig. 1(b)]. As we show below, such a dual-species configuration facilitates both parallel and efficient simulations of the desired multibody interactions.

Simulation of the quantum evolution is then realized by a Trotterized sequence $e^{-iH\tau} \approx \prod_p e^{-iH_p\tau} + \mathcal{O}(\tau^2)$, where $H = \sum_p H_p$ and each H_p is a collection of mutually commuting terms that can be executed in a parallel and system-size independent manner. With the physical system sketched above, arbitrary combinations of the simplified Hamiltonians $\{H_1, H_{\mathbb{Z}_2^a}, H_{\mathbb{Z}_2^{ab}}, H_{(\mathbb{Z}_2^a\times\mathbb{Z}_2^b)^\pm}\}$ in Table I (bold terms) can be efficiently simulated. Expressing such a combination in the generic form Eq. (1), first, the on-site evolutions $e^{-iP_i\tau}$ involving up to three-body interactions can be realized by three types of phase gates in few steps: single-qubit phase gate $U_{\mathrm{P}}(\phi) = e^{-i\phi Q_i^{\mathrm{I}}}$, two-qubit controlled phase gate $U_{\mathrm{CP}}(\phi) = e^{-i\phi Q_i^{\mathrm{I}} Q_i^{\alpha}}$ $(\alpha = \mathrm{II}, \mathrm{III})$, and three-qubit controlled phase gate $U_{\mathrm{CCP}}(\phi) = e^{-i\phi Q_i^{\mathrm{I}} Q_i^{\mathrm{II}} Q_i^{\mathrm{III}}}$, where $Q = (\mathbb{I} + Z)/2 = |0\rangle\langle 0|$. As data qubits sitting on different sites are outside the blockade radius, the operation $e^{-i\sum_i P_i\tau}$ can be parallelized [73,74]. Second, the two-site evolution $e^{-iV_{i,i+1}\tau}$ containing up to four-body plaquette interactions $U_{\square}(\phi) = \exp(-i\phi \mathcal{O}_i^{\mathrm{II}} \mathcal{O}_{i+1}^{\mathrm{II}} \mathcal{O}_{i+1}^{\mathrm{III}} \mathcal{O}_i^{\mathrm{III}})$ with $\mathcal{O}_j^{\alpha} \in \{\mathbb{I}, X, Y, Z\}_j^{\alpha}$ can be constructed from a multiqubit Z gate controlled by an ancillary qubit [75–77]. In such a construction, the ancillary qubit is only temporarily entangled with data qubits and can be traced out from the dynamics after completion of the gate operation (see SM [49]). Since each data qubit is only affected by its two closest ancillary qubits, this operation can be executed in just two steps $e^{-i\sum_i V_{2i-1,2i}\tau}$ and $e^{-i\sum_i V_{2i,2i+1}\tau}$. The stroboscopic application of the on-site and the intersite evolution then composes a Trotterization, realizing the desired many-body evolution [see Fig. 1(c)].

To show the performance of our scheme, we study a quantum annealing dynamics, in which the Hamiltonian is adiabatically varied in the form of Eq. (12) with a time-dependent $\lambda = t/T$. The annealing time $T \sim 1/\Delta E \propto L$ (where ΔE is the energy gap and L the number of lattice sites) scales linearly with the system size [49], as expected for $(1+1)$d CFTs [78,79]. Here, we consider two interesting interpolations: H_1 to $H_{\mathbb{Z}_2^{ab}}$ and H_1 to $H_{(\mathbb{Z}_2^a\times\mathbb{Z}_2^b)^-}$. The former establishes the transition from a trivial paramagnetic phase with spins on different sites independently aligned, to a symmetry-breaking phase where spins at $\{\mathrm{II}_i, \mathrm{III}_i\}$ form a Bell pair and are ordered in a correlated manner [see Fig. 2(a)]. In this phase, the noninvertible symmetry $\mathcal{S}_E$ is spontaneously broken, while all grouplike symmetries $(\mathcal{S}_{1_a}, \mathcal{S}_{1_c}, \mathcal{S}_{1_{ca}})$ are preserved. The second interpolation realizes a transition from the trivial phase to an SPT phase featuring a cluster-state-like ground state [see Fig. 2(b)]. When preparing the ground state with a digital annealing, there are two types of errors: the diabatic error induced by leakages from the ground-state manifold and the Trotter error caused by a finite step size τ. As shown in Figs. 2(c) and 2(d), the Trotter errors are small even for a very large Trotter step $\tau \sim 1$. To experimentally probe these transitions, one can measure local [34] and string [39,80] order parameters $\mathcal{O}_{\mathrm{loc}}$ and $\mathcal{O}_{\mathrm{str}}$ associated with each nontrivial phase [81] [see Figs. 2(a) and 2(b)]. We note that by increasing the annealing time T ($\propto$ total number of gates), the diabatic error can be reduced, and the order parameters exhibit sharper transitions.

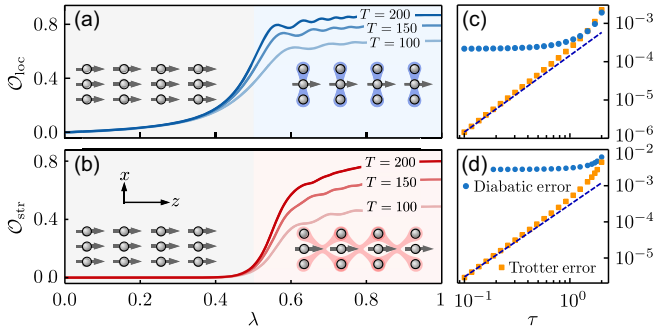


FIG. 2. (a) and (b) show the evolution of the local and string order parameters $\mathcal{O}_{\mathrm{loc}}$ and $\mathcal{O}_{\mathrm{str}}$ for the annealing across the phase transition Trivial $\to$ $\mathsf{Rep}(D_8)/(\mathbb{Z}_2\times\mathbb{Z}_2)$ SSB and Trivial $\to$ SPT, respectively. The results are obtained by time-evolving block decimation with $L = 18$ sites (54 data qubits) and $\tau = 1$. (c) and (d) show the errors in (a) and (b) as a function of the step size τ with $L = 6$. The dashed curves are polynomial fits ($\propto \tau^2$) to the Trotter errors. In (a), symmetry-breaking defects are included at the boundaries to select one of the degenerate ground states.

Generalization—While the current configuration supports the exploration of the first five regimes in Table I, which already include an example of each type of phase except the $\mathsf{Rep}(D_8)$ SSB, a simple generalization can reach all possible phases emerging from the $\mathsf{Rep}(D_8)$ symmetry, specifically the $\mathsf{Rep}(D_8)$ SSB. This is a gapped phase where the $\mathsf{Rep}(D_8)$ categorical symmetry is completely broken, and whose ground-state degeneracy cannot be explained by any (UV or IR) grouplike symmetry. The phase transition between a $\mathbb{Z}_2\times\mathbb{Z}_2$ SSB, e.g., $H_{(\mathbb{Z}_2^a\times\mathbb{Z}_2^b)^+}$, to the $\mathsf{Rep}(D_8)$ SSB $H_{(D_8)^+}$ is particularly noteworthy since it is an Ising intrinsically gapless SSB [10]: it has three gapless ground states (also called "universes"), each of which is the Ising CFT, that are related to each other by a spontaneously broken Ising categorical subsymmetry of $\mathsf{Rep}(D_8)$ [82] (see Fig. 3). It is "intrinsically" gapless since no gapped phases exhibit this symmetry-breaking pattern.

To achieve the simulation for this general case, one can include a different Rydberg state $|r'\rangle$ when implementing the two-site evolution. This Rydberg state should support a highly asymmetric blockade, in which data qubits themselves are completely noninteracting (even the nearest neighbors), but can be blockaded by the neighboring

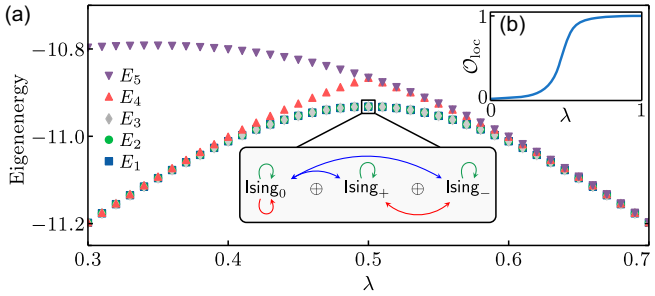


FIG. 3. Characterization of the quantum phase transition $(\mathbb{Z}_2 \times \mathbb{Z}_2)$ SSB $\to$ Rep(D_8) SSB. (a) and (b) show the spectrum (lowest five eigenenergies) and the order parameter $\mathcal{O}_{\rm loc} = \sum_i X_i^{\rm I}/L$ as a function of λ. The results are obtained by exact diagonalization with $L = 6$ sites (18 qubits). In (b), a symmetry-breaking perturbation $-0.01 \sum_i X_i^{\rm I}$ is applied.

ancillary atom, described by a constrained Hamiltonian $(\Omega_{r'}/2)(\mathbb{I}_{\rm c} - |r'\rangle\langle r'|_{\rm c}) \otimes (\Sigma_n |r'\rangle\langle 0|_n + {\rm H.c.})$, where every data qubit $(n = 1, \ldots, 6)$ in a given plaquette can be excited to the Rydberg state $|r'\rangle_n$ if the ancillary qubit is not in the Rydberg state $|r'\rangle_{\rm c}$. Then, using the same gate sequence [49] for the two-site evolution as before, arbitrary six-body interactions $U'_{\square}(\phi) = \exp(-{\rm i}\phi \mathcal{O}_i^{\rm I}\mathcal{O}_{i+1}^{\rm I}\mathcal{O}_i^{\rm II}\mathcal{O}_{i+1}^{\rm II}\mathcal{O}_i^{\rm III}\mathcal{O}_{i+1}^{\rm III})$ with $\mathcal{O}_j^{\alpha} \in \{\mathbb{I}, X, Y, Z\}_j^{\alpha}$ within each plaquette can be engineered. Such a highly asymmetric regime can be achieved by utilizing the anisotropy of the Rydberg interaction [83] or microwave dressing [84].

Conclusion and outlook—In summary, we have constructed a spin-chain model realizing all gapped phases and second-order phase transitions for the Rep(D_8) categorical symmetry, and provided a concrete proposal for implementing the model in a Rydberg quantum simulator. Based on the current scheme, it is possible to increase the circuit depth, as both the execution time and the robustness of each elementary gate can be improved by optimal control methods [85,86]. In addition to the dual-species scheme, one may also use a linear-chain configuration and coherently rearrange atomic qubits [87] to establish the multibody interaction, e.g., using the globally driving scheme to realize the four-body interaction [88]. While we focus on a digital implementation here, developing analog simulation schemes represents an interesting route as well.

The physical implementation presented here serves as a versatile framework for simulating a wide range of categorical symmetries, such as Rep(S_3) noninvertible symmetries [89–91] and spin models in higher dimensions. Indeed, for higher categorical symmetries [92–94] in $(2+1)$d and $(3+1)$d, lattice models have been developed recently in [95–99], giving rise to novel phases of matter, e.g., Refs. [100–105]. Extending the framework discussed here to higher dimensions would naturally align with these developments and presents an exciting challenge for experimental realization in neutral-atom systems as well as other quantum simulation platforms, such as superconducting circuits [106] and trapped ions [107].

Acknowledgments—We thank Lea Bottini, Luisa Eck, Paul Fendley, Yuhan Gai, Camillo Imbimbo, Dan Pajer, Zhongda Zeng, Klaus Mølmer, and Torsten V. Zache for discussions at various stages of this work and Lakshya Bhardwaj for initial collaboration. The work of S. S. N. and A. W. is supported by the UKRI Frontier Research Grant, underwriting the ERC Advanced Grant "Generalized Symmetries in Quantum Field Theory and Quantum Gravity." A. T. is funded by Villum Fonden Grant No. VIL60714. Work in Innsbruck is supported by the European Union's Horizon Europe research and innovation program under Grant Agreement No. 101113690 (PASQuanS2.1), the ERC Starting grant QARA (Grant No. 101041435), and the Austrian Science Fund (FWF) (Grant No. DOI 10.55776/COE1).

Data availability—The data that support the findings of this article are openly available [108].

[1] S. Schafer-Nameki, ICTP lectures on (non-)invertible generalized symmetries, Phys. Rep. **1063**, 1 (2024).
[2] S.-H. Shao, What's done cannot be undone: TASI lectures on noninvertible symmetry, arXiv:2308.00747.
[3] L. Bhardwaj and S. Schafer-Nameki, Generalized charges, part II: Noninvertible symmetries and the symmetry TFT, arXiv:2305.17159.
[4] L. Bhardwaj, L. E. Bottini, D. Pajer, and S. Schafer-Nameki, Categorical Landau paradigm for gapped phases, Phys. Rev. Lett. **133**, 161601 (2024).
[5] L. Bhardwaj, L. E. Bottini, D. Pajer, and S. Schäfer-Nameki, Gapped phases with noninvertible symmetries: $(1+1)$d, SciPost Phys. **18**, 032 (2025).
[6] L. Bhardwaj, L. E. Bottini, D. Pajer, and S. Schafer-Nameki, The club sandwich: Gapless phases and phase transitions with noninvertible symmetries, SciPost Phys. **18**, 156 (2025).
[7] A. Chatterjee and X.-G. Wen, Holographic theory for continuous phase transitions: Emergence and symmetry protection of gaplessness, Phys. Rev. B **108**, 075105 (2023).
[8] R. Wen and A. C. Potter, Classification of $1+1$D gapless symmetry protected phases via topological holography, Phys. Rev. B **111**, 115161 (2025).
[9] S.-J. Huang and M. Cheng, Topological holography, quantum criticality, and boundary states, SciPost Phys. **18**, 213 (2025).
[10] L. Bhardwaj, D. Pajer, S. Schafer-Nameki, and A. Warman, Hasse diagrams for gapless SPT and SSB phases with non-invertible symmetries, SciPost Phys. **19**, 113 (2025).
[11] W. Ji and X.-G. Wen, Categorical symmetry and noninvertible anomaly in symmetry-breaking and topological phase transitions, Phys. Rev. Res. **2**, 033417 (2020).
[12] D. Gaiotto and J. Kulp, Orbifold groupoids, J. High Energy Phys. 02 (2021) 132.
[13] F. Apruzzi, F. Bonetti, I. n. García Etxebarria, S. S. Hosseini, and S. Schafer-Nameki, Symmetry TFTs from string theory, Commun. Math. Phys. **402**, 895 (2023).

[14] D. S. Freed, G. W. Moore, and C. Teleman, Topological symmetry in quantum field theory, arXiv:2209.07471.

[15] H. Moradi, S. F. Moosavian, and A. Tiwari, Topological holography: Towards a unification of Landau and beyond-Landau physics, SciPost Phys. Core **6**, 066 (2023).

[16] For gapped phases, an alternative approach uses module categories in [17].

[17] R. Thorngren and Y. Wang, Fusion category symmetry. Part I. Anomaly in-flow and gapped phases, J. High Energy Phys. 04 (2024) 132.

[18] T.-C. Huang, Y.-H. Lin, K. Ohmori, Y. Tachikawa, and M. Tezuka, Numerical evidence for a Haagerup conformal field theory, Phys. Rev. Lett. **128**, 231603 (2022).

[19] R. Vanhove, L. Lootens, M. Van Damme, R. Wolf, T. J. Osborne, J. Haegeman, and F. Verstraete, Critical lattice model for a Haagerup conformal field theory, Phys. Rev. Lett. **128**, 231602 (2022).

[20] L. E. Bottini and S. Schafer-Nameki, Construction of a gapless phase with Haagerup symmetry, Phys. Rev. Lett. **134**, 191602 (2025).

[21] The input data that determines the Hilbert space is ($\mathcal{C}$, $\mathcal{M}$, $\rho \in \mathcal{C}$), where $\mathcal{C}$ is a fusion category, $\mathcal{M}$ is a $\mathcal{C}$-module category and $\mathcal{S} = \mathcal{C}^*_{\mathcal{M}}$ is the actual symmetry category.

[22] A. Feiguin, S. Trebst, A. W. W. Ludwig, M. Troyer, A. Kitaev, Z. Wang, and M. H. Freedman, Interacting anyons in topological quantum liquids: The golden chain, Phys. Rev. Lett. **98**, 160409 (2007).

[23] D. Aasen, R. S. K. Mong, and P. Fendley, Topological defects on the lattice I: The Ising model, J. Phys. A **49**, 354001 (2016).

[24] D. Aasen, P. Fendley, and R. S. K. Mong, Topological defects on the lattice: Dualities and degeneracies, arXiv:2008.08598.

[25] I. Cong, M. Cheng, and Z. Wang, Hamiltonian and algebraic theories of gapped boundaries in topological phases of matter, Commun. Math. Phys. **355**, 645 (2017).

[26] M. Buican and A. Gromov, Anyonic chains, topological defects, and conformal field theory, Commun. Math. Phys. **356**, 1017 (2017).

[27] K. Inamura, Topological field theories and symmetry protected topological phases with fusion category symmetries, J. High Energy Phys. 05 (2021) 204.

[28] L. Lootens, C. Delcamp, G. Ortiz, and F. Verstraete, Dualities in one-dimensional quantum lattice models: Symmetric Hamiltonians and matrix product operator intertwiners, PRX Quantum **4**, 020357 (2023).

[29] L. Bhardwaj, L. E. Bottini, S. Schafer-Nameki, and A. Tiwari, Lattice models for phases and transitions with noninvertible symmetries, arXiv:2405.05964.

[30] A. Browaeys and T. Lahaye, Many-body physics with individually controlled Rydberg atoms, Nat. Phys. **16**, 132 (2020).

[31] X. Wu, X. Liang, Y. Tian, F. Yang, C. Chen, Y.-C. Liu, M. K. Tey, and L. You, A concise review of Rydberg atom based quantum computation and quantum simulation, Chin. Phys. B **30**, 020305 (2021).

[32] A. M. Kaufman and K.-K. Ni, Quantum science with optical tweezer arrays of ultracold atoms and molecules, Nat. Phys. **17**, 1324 (2021).

[33] M. Morgado and S. Whitlock, Quantum simulation and computing with Rydberg-interacting qubits, AVS Quantum Sci. **3**, 023501 (2021).

[34] H. Bernien, S. Schwartz, A. Keesling, H. Levine, A. Omran, H. Pichler, S. Choi, A. S. Zibrov, M. Endres, M. Greiner *et al.*, Probing many-body dynamics on a 51-atom quantum simulator, Nature (London) **551**, 579 (2017).

[35] A. Keesling, A. Omran, H. Levine, H. Bernien, H. Pichler, S. Choi, R. Samajdar, S. Schwartz, P. Silvi, S. Sachdev, P. Zoller, M. Endres, M. Greiner, V. Vuletić, and M. D. Lukin, Quantum Kibble–Zurek mechanism and critical dynamics on a programmable Rydberg simulator, Nature (London) **568**, 207 (2019).

[36] P. Scholl, M. Schuler, H. J. Williams, A. A. Eberharter, D. Barredo, K.-N. Schymik, V. Lienhard, L.-P. Henry, T. C. Lang, T. Lahaye, A. M. Läuchli, and A. Browaeys, Quantum simulation of 2d antiferromagnets with hundreds of Rydberg atoms, Nature (London) **595**, 233 (2021).

[37] S. Ebadi, T. T. Wang, H. Levine, A. Keesling, G. Semeghini, A. Omran, D. Bluvstein, R. Samajdar, H. Pichler, W. W. Ho, S. Choi, S. Sachdev, M. Greiner, V. Vuletić, and M. D. Lukin, Quantum phases of matter on a 256-atom programmable quantum simulator, Nature (London) **595**, 227 (2021).

[38] C. Chen, G. Bornet, M. Bintz, G. Emperauger, L. Leclerc, V. S. Liu, P. Scholl, D. Barredo, J. Hauschild, S. Chatterjee *et al.*, Continuous symmetry breaking in a two-dimensional Rydberg array, Nature (London) **616**, 691 (2023).

[39] G. Semeghini, H. Levine, A. Keesling, S. Ebadi, T. T. Wang, D. Bluvstein, R. Verresen, H. Pichler, M. Kalinowski, R. Samajdar, A. Omran, S. Sachdev, A. Vishwanath, M. Greiner, V. Vuletić, and M. D. Lukin, Probing topological spin liquids on a programmable quantum simulator, Science **374**, 1242 (2021).

[40] K. Singh, C. E. Bradley, S. Anand, V. Ramesh, R. White, and H. Bernien, Mid-circuit correction of correlated phase errors using an array of spectator qubits, Science **380**, 1265 (2023).

[41] S. Anand, C. E. Bradley, R. White, V. Ramesh, K. Singh, and H. Bernien, A dual-species Rydberg array, Nat. Phys. **20**, 1744 (2024).

[42] S. Seifnashri and S.-H. Shao, Cluster state as a non-invertible symmetry-protected topological phase, Phys. Rev. Lett. **133**, 116601 (2024).

[43] L. Li, R.-Z. Huang, and W. Cao, Noninvertible symmetry-enriched quantum critical point, Phys. Rev. B **112**, L081113 (2025).

[44] C. Meng, X. Yang, T. Lan, and Z. Gu, Noninvertible SPTs: An on-site realization of $(1+1)$d anomaly-free fusion category symmetry, arXiv:2412.20546.

[45] For the expert reader, we choose the categorical input data, $\mathcal{C} = \mathsf{Vec}_{D_8}$, $\mathcal{M} = \mathsf{Vec}$, $\rho = \oplus_{g \in D_8} g$, so that the symmetry of the model is $\mathcal{S} = \mathcal{C}^*_{\mathcal{M}} = \mathsf{Rep}(D_8)$.

[46] $H_{(F,\beta)}$ is Hermitian as the projectors are and $(L^{\mathsf{f}}_{\beta})^{\dagger} = L^{\mathsf{f}^{-1}}_{\beta}$, $(R^{\mathsf{f}}_{\beta})^{\dagger} = R^{\mathsf{f}^{-1}}_{\beta}$, and we sum over $f \in F$ where F is a group. One can write equivalent Hamiltonians by summing only over generators of F and their inverses.

[47] The operators L_g, R_g, Z_Γ for dihedral groups presented as $\mathbb{Z}_N \rtimes \mathbb{Z}_2$ can be found in Appendix B of [48].

[48] V. V. Albert, D. Aasen, W. Xu, W. Ji, J. Alicea, and J. Preskill, Spin chains, defects, and quantum wires for the quantum-double edge, arXiv:2111.12096.

[49] See Supplemental Material at http://link.aps.org/supplemental/10.1103/249m-m8wq for $\mathsf{Rep}(D_8)$ symmetry multiplets, derivation of ground states of the Hamiltonians, further information on phase transitions, and details on the experimental scheme, which includes Ref. [50–62].

[50] D. Tambara and S. Yamagami, Tensor categories with fusion rules of self-duality for finite Abelian groups, J. Algebra **209**, 692 (1998).

[51] V. Ostrik, Module categories over the Drinfeld double of a finite group, arXiv:math/0202130.

[52] M. Iqbal *et al.*, Non-Abelian topological order and anyons on a trapped-ion processor, Nature (London) **626**, 505 (2024).

[53] Y.-H. Lin, M. Okada, S. Seifnashri, and Y. Tachikawa, Asymptotic density of states in 2d CFTs with noninvertible symmetries, J. High Energy Phys. 03 (2023) 094.

[54] L. Bhardwaj and S. Schafer-Nameki, Generalized charges, part I: Invertible symmetries and higher representations, SciPost Phys. **16**, 093 (2024).

[55] L. Bhardwaj, L. E. Bottini, S. Schafer-Nameki, and A. Tiwari, Noninvertible symmetry webs, SciPost Phys. **15**, 160 (2023).

[56] D. Pérez-García, M. M. Wolf, M. Sanz, F. Verstraete, and J. I. Cirac, String order and symmetries in quantum spin lattices, Phys. Rev. Lett. **100**, 167202 (2008).

[57] F. Pollmann and A. M. Turner, Detection of symmetry-protected topological phases in one dimension, Phys. Rev. B **86**, 125441 (2012).

[58] H. Moradi, O. M. Aksoy, J. H. Bardarson, and A. Tiwari, Symmetry fractionalization, mixed-anomalies and dualities in quantum spin models with generalized symmetries, SciPost Phys. **18**, 097 (2025).

[59] T. Kennedy and H. Tasaki, Hidden $Z2 \times Z2$ symmetry breaking in haldane-gap antiferromagnets, Phys. Rev. B **45**, 304 (1992).

[60] T. Kennedy and H. Tasaki, Hidden symmetry breaking and the haldane phase in $s = 1$ quantum spin chains, Commun. Math. Phys. **147**, 431 (1992).

[61] R. Trivedi, A. F. Rubio, and J. I. Cirac, Quantum advantage and stability to errors in analogue quantum simulators, Nat. Commun. **15**, 6507 (2024).

[62] S. De Léséleuc, D. Barredo, V. Lienhard, A. Browaeys, and T. Lahaye, Analysis of imperfections in the coherent optical excitation of single atoms to Rydberg states, Phys. Rev. A **97**, 053803 (2018).

[63] J. Zeiher, J.-y. Choi, A. Rubio-Abadal, T. Pohl, R. Van Bijnen, I. Bloch, and C. Gross, Coherent many-body spin dynamics in a long-range interacting Ising chain, Phys. Rev. X **7**, 041063 (2017).

[64] P. Scholl, A. L. Shaw, R. B.-S. Tsai, R. Finkelstein, J. Choi, and M. Endres, Erasure conversion in a high-fidelity Rydberg quantum simulator, Nature (London) **622**, 273 (2023).

[65] L.-M. Steinert, P. Osterholz, R. Eberhard, L. Festa, N. Lorenz, Z. Chen, A. Trautmann, and C. Gross, Spatially tunable spin interactions in neutral atom arrays, Phys. Rev. Lett. **130**, 243001 (2023).

[66] K. Kim, F. Yang, K. Mølmer, and J. Ahn, Realization of an extremely anisotropic Heisenberg magnet in Rydberg atom arrays, Phys. Rev. X **14**, 011025 (2024).

[67] H. Levine, A. Keesling, G. Semeghini, A. Omran, T. T. Wang, S. Ebadi, H. Bernien, M. Greiner, V. Vuletić, H. Pichler *et al.*, Parallel implementation of high-fidelity multiqubit gates with neutral atoms, Phys. Rev. Lett. **123**, 170503 (2019).

[68] S. Ma, G. Liu, P. Peng, B. Zhang, S. Jandura, J. Claes, A. P. Burgers, G. Pupillo, S. Puri, and J. D. Thompson, High-fidelity gates and mid-circuit erasure conversion in an atomic qubit, Nature (London) **622**, 279 (2023).

[69] A. Cao, W. J. Eckner, T. Lukin Yelin, A. W. Young, S. Jandura, L. Yan, K. Kim, G. Pupillo, J. Ye, N. Darkwah Oppong *et al.*, Multi-qubit gates and Schrödinger cat states in an optical clock, Nature (London) **634**, 315 (2024).

[70] N. Maskara, S. Ostermann, J. Shee, M. Kalinowski, A. M. Gomez, R. A. Bravo, D. S. Wang, A. I. Krylov, N. Y. Yao, M. Head-Gordon *et al.*, Programmable simulations of molecules and materials with reconfigurable quantum processors, arXiv:2312.02265.

[71] D. Jaksch, J. I. Cirac, P. Zoller, S. L. Rolston, R. Côté, and M. D. Lukin, Fast quantum gates for neutral atoms, Phys. Rev. Lett. **85**, 2208 (2000).

[72] A. Omran, H. Levine, A. Keesling, G. Semeghini, T. T. Wang, S. Ebadi, H. Bernien, A. S. Zibrov, H. Pichler, S. Choi, J. Cui, M. Rossignolo, P. Rembold, S. Montangero, T. Calarco, M. Endres, M. Greiner, V. Vuletić, and M. D. Lukin, Generation and manipulation of Schrödinger cat states in Rydberg atom arrays, Science **365**, 570 (2019).

[73] S. J. Evered, D. Bluvstein, M. Kalinowski, S. Ebadi, T. Manovitz, H. Zhou, S. H. Li, A. A. Geim, T. T. Wang, N. Maskara *et al.*, High-fidelity parallel entangling gates on a neutral-atom quantum computer, Nature (London) **622**, 268 (2023).

[74] D. Bluvstein, S. J. Evered, A. A. Geim, S. H. Li, H. Zhou, T. Manovitz, S. Ebadi, M. Cain, M. Kalinowski, D. Hangleiter *et al.*, Logical quantum processor based on reconfigurable atom arrays, Nature (London) **626**, 58 (2024).

[75] H. Weimer, M. Müller, I. Lesanovsky, P. Zoller, and H. P. Büchler, A Rydberg quantum simulator, Nat. Phys. **6**, 382 (2010).

[76] H. Weimer, M. Müller, H. P. Büchler, and I. Lesanovsky, Digital quantum simulation with Rydberg atoms, Quantum Inf. Process. **10**, 885 (2011).

[77] A. Bohrdt, A. Omran, E. Demler, S. Gazit, and F. Grusdt, Multiparticle interactions for ultracold atoms in optical tweezers: Cyclic ring-exchange terms, Phys. Rev. Lett. **124**, 073601 (2020).

[78] J. L. Cardy, Effect of boundary conditions on the operator content of two-dimensional conformally invariant theories, Nucl. Phys. B **275**, 200 (1986).

[79] M. Oshikawa, Universal finite-size gap scaling of the quantum Ising chain, arXiv:1910.06353.

[80] S. De Léséleuc, V. Lienhard, P. Scholl, D. Barredo, S. Weber, N. Lang, H. P. Büchler, T. Lahaye, and A. Browaeys, Observation of a symmetry-protected topological phase of interacting bosons with Rydberg atoms, Science **365**, 775 (2019).

[81] The local and string order parameters here are given by $\mathcal{O}_{\mathrm{loc}} = \Sigma_i \langle X^{\mathrm{II}} X^{\mathrm{III}} \rangle_i / L$ and $\mathcal{O}_{\mathrm{str}} = \langle X^{\mathrm{II}}_i X^{\mathrm{III}}_{i+1} [\Pi_{k=1}^{l-2} (Z^{\mathrm{II}} Z^{\mathrm{III}})_{i+k}] X^{\mathrm{II}}_{i+l-2} X^{\mathrm{III}}_{i+l-1} \rangle$. In the time-evolving block decimation simulation, we consider the string at the center of the system with a length $l = 6$.

[82] There is $\sqrt{2}$ "relative Euler term" between Ising_0 and each of $\mathsf{Ising}_{\pm}$, since E has quantum dimension 2, whereas the Ising noninvertible symmetry has quantum dimension $\sqrt{2}$.

[83] D. Barredo, S. Ravets, H. Labuhn, L. Béguin, A. Vernier, F. Nogrette, T. Lahaye, and A. Browaeys, Demonstration of a strong Rydberg blockade in three-atom systems with anisotropic interactions, Phys. Rev. Lett. **112**, 183002 (2014).

[84] J. T. Young, P. Bienias, R. Belyansky, A. M. Kaufman, and A. V. Gorshkov, Asymmetric blockade and multiqubit gates via dipole-dipole interactions, Phys. Rev. Lett. **127**, 120501 (2021).

[85] S. Jandura and G. Pupillo, Time-optimal two-and three-qubit gates for Rydberg atoms, Quantum **6**, 712 (2022).

[86] C. Fromonteil, R. Tricarico, F. Cesa, and H. Pichler, Hamilton-Jacobi-Bellman equations for Rydberg-blockade processes, Phys. Rev. Res. **6**, 033333 (2024).

[87] D. Bluvstein, H. Levine, G. Semeghini, T. T. Wang, S. Ebadi, M. Kalinowski, A. Keesling, N. Maskara, H. Pichler, M. Greiner *et al.*, A quantum processor based on coherent transport of entangled atom arrays, Nature (London) **604**, 451 (2022).

[88] C. Dlaska, K. Ender, G. B. Mbeng, A. Kruckenhauser, W. Lechner, and R. van Bijnen, Quantum optimization via four-body Rydberg gates, Phys. Rev. Lett. **128**, 120503 (2022).

[89] L. Eck and P. Fendley, Critical lines and ordered phases in a Rydberg-blockade ladder, Phys. Rev. B **108**, 125135 (2023).

[90] L. Bhardwaj, L. E. Bottini, S. Schafer-Nameki, and A. Tiwari, Illustrating the categorical Landau paradigm in lattice models, Phys. Rev. B **111**, 054432 (2025).

[91] A. Chatterjee, Ö. M. Aksoy, and X.-G. Wen, Quantum phases and transitions in spin chains with noninvertible symmetries, SciPost Phys. **17**, 115 (2024).

[92] J. Kaidi, K. Ohmori, and Y. Zheng, Kramers-Wannier-like duality defects in $(3+1)$D gauge theories, Phys. Rev. Lett. **128**, 111601 (2022).

[93] Y. Choi, C. Cordova, P.-S. Hsin, H. T. Lam, and S.-H. Shao, Noninvertible duality defects in $3+1$ dimensions, Phys. Rev. D **105**, 125016 (2022).

[94] L. Bhardwaj, L. E. Bottini, S. Schafer-Nameki, and A. Tiwari, Noninvertible higher-categorical symmetries, SciPost Phys. **14**, 007 (2023).

[95] C. Delcamp and A. Tiwari, Higher categorical symmetries and gauging in two-dimensional spin systems, SciPost Phys. **16**, 110 (2024).

[96] K. Inamura and K. Ohmori, Fusion surface models: $2+1$d lattice models from fusion 2-categories, SciPost Phys. **16**, 143 (2024).

[97] L. Eck and P. Fendley, Generalizations of Kitaev's honeycomb model from braided fusion categories, SciPost Phys. **18**, 170 (2025).

[98] P. Gorantla, S.-H. Shao, and N. Tantivasadakarn, Tensor networks for noninvertible symmetries in $3+1$d and beyond, Phys. Rev. X **15**, 041006 (2025).

[99] K. Inamura, S.-J. Huang, A. Tiwari, and S. Schafer-Nameki, $(2+1)$d lattice models and tensor networks for gapped phases with categorical symmetry, arXiv:2506.09177.

[100] A. Antinucci, C. Copetti, and S. Schafer-Nameki, SymTFT for $(3+1)$d gapless SPTs and obstructions to confinement, SciPost Phys. **18**, 114 (2025).

[101] L. Bhardwaj, D. Pajer, S. Schäfer-Nameki, A. Tiwari, A. Warman, and J. Wu, Gapped phases in $(2+1)$d with noninvertible symmetries: Part I, SciPost Phys. **19**, 056 (2025).

[102] R. Wen, String condensation and topological holography for $2+1$D gapless SPT, arXiv:2408.05801.

[103] Y. Choi, Y. Sanghavi, S.-H. Shao, and Y. Zheng, Noninvertible and higher-form symmetries in $2+1$d lattice gauge theories, SciPost Phys. **18**, 008 (2025).

[104] L. Bhardwaj, S. Schafer-Nameki, A. Tiwari, and A. Warman, Gapped phases in $(2+1)$d with noninvertible symmetries: Part II, arXiv:2502.20440.

[105] L. Bhardwaj, Y. Gai, S.-J. Huang, K. Inamura, S. Schafer-Nameki, A. Tiwari, and A. Warman, Gapless phases in $(2+1)$d with noninvertible symmetries, arXiv:2503.12699.

[106] H.-L. Huang, D. Wu, D. Fan, and X. Zhu, Superconducting quantum computing: A review, Sci. China Inf. Sci. **63**, 1 (2020).

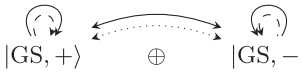
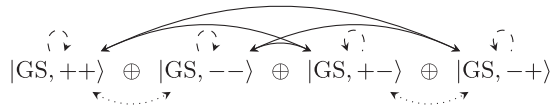
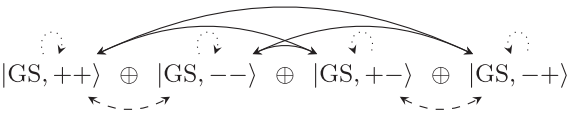
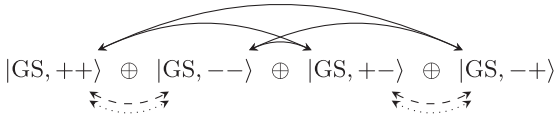
[107] C. Monroe, W. C. Campbell, L.-M. Duan, Z.-X. Gong, A. V. Gorshkov, P. W. Hess, R. Islam, K. Kim, N. M. Linke, G. Pagano *et al.*, Programmable quantum simulations of spin systems with trapped ions, Rev. Mod. Phys. **93**, 025001 (2021).

[108] A. Warman and F. Yang, Dataset for categorical symmetries in spin models with atom arrays, 10.5281/zenodo.16963608 (2025).

End Matter

Summary table of $\mathsf{Rep}(D_8)$*-symmetric gapped phases*—Table I summarizes all $\mathsf{Rep}(D_8)$-symmetric gapped phases, with their Hamiltonians, number of ground states as well as the symmetry action, including the noninvertible generator E satisfying (3). They are either symmetry protected topological (SPT) or spontaneous symmetry breaking (SSB) phases for particular subsymmetries of $\mathsf{Rep}(D_8)$.

TABLE I. All gapped phases for the benchmark system with $\mathsf{Rep}(D_8)$ symmetry, showing the type of phase, i.e. SSB (spontaneously broken symmetry) and SPT (symmetry protected topological phase). For each phase we write the commuting projector Hamiltonian of the spin model, realized on $(\mathbb{C}^2_{\mathrm{I}} \otimes \mathbb{C}^2_{\mathrm{II}} \otimes \mathbb{C}^2_{\mathrm{III}})^L$ and the number of ground states (GS) with the action of the categorical symmetry. We depict the $\mathsf{Rep}(D_8)$ symmetry action on the ground states as follows: 1_c as dotted, 1_a as dashed, (their product is $1_{ca} = 1_c \otimes 1_a$) and the non-invertible symmetry E as solid. We use a single line for the full $\mathsf{Rep}(D_8)$. The first five Hamiltonians can be simplified by first applying the $-(\mathbb{I} + Z^{\mathrm{I}})_i/2$ projector: they then reduce to the bold terms, which can be implemented in our experimental proposal based on dual-species atom arrays. The other Hamiltonians require a slight generalization. The colored version of this Table can be found in Supplemental Material [49].

Phase type	Hamiltonian and ground states with $\mathsf{Rep}(D_8)$ action
Trivial	$\boldsymbol{H_1 = -\sum_i [\mathbb{I} + \frac{1}{8}(\mathbb{I}+\boldsymbol{Z^{\mathrm{I}}})(\mathbb{I}+\boldsymbol{Z^{\mathrm{II}}})(\mathbb{I}+\boldsymbol{Z^{\mathrm{III}}})]_i} \simeq -\sum_i [\mathbb{I} + \frac{1}{4}(\mathbb{I}+\boldsymbol{Z^{\mathrm{I}}})(\boldsymbol{Z^{\mathrm{II}}}+\boldsymbol{Z^{\mathrm{III}}})]_i$, $\lvert \mathrm{GS}\rangle \circlearrowleft$
$\mathbb{Z}_2$ SSB	$\boldsymbol{H_{\mathbb{Z}_2^a} = -\frac{1}{2}\sum_i [\mathbb{I}_i\mathbb{I}_{i+1} + \frac{1}{2}(\mathbb{I}+Z^{\mathrm{I}})_i \boldsymbol{X_i^{\mathrm{II}} X_{i+1}^{\mathrm{II}}} + \frac{1}{2}(\mathbb{I}-Z^{\mathrm{I}})_i X_i^{\mathrm{III}} X_{i+1}^{\mathrm{II}}] - \frac{1}{4}\sum_i [(\mathbb{I}+\boldsymbol{Z^{\mathrm{I}}})(\mathbb{I}+\boldsymbol{Z^{\mathrm{III}}})]_i}$ 
$[\mathsf{Rep}(D_8)/(\mathbb{Z}_2 \times \mathbb{Z}_2)]$ SSB	$\boldsymbol{H_{\mathbb{Z}_2^{ab}} = -\frac{1}{2}\sum_i [\mathbb{I}_i\mathbb{I}_{i+1} + (\boldsymbol{X^{\mathrm{II}}X^{\mathrm{III}}})_i (\boldsymbol{X^{\mathrm{II}}X^{\mathrm{III}}})_{i+1}] - \frac{1}{4}\sum_i [(\mathbb{I}+\boldsymbol{Z^{\mathrm{I}}})(\mathbb{I}+\boldsymbol{Z^{\mathrm{II}}Z^{\mathrm{III}}})]_i}$ 
$\mathbb{Z}_2 \times \mathbb{Z}_2$ SSB	$\boldsymbol{H_{(\mathbb{Z}_2^a \times \mathbb{Z}_2^b)^+} \simeq -\frac{1}{2}\sum_i [\frac{1}{2}(\mathbb{I}+Z^{\mathrm{I}})_i (\boldsymbol{X_i^{\mathrm{II}} X_{i+1}^{\mathrm{II}} + X_i^{\mathrm{III}} X_{i+1}^{\mathrm{III}}})} + \frac{1}{2}(\mathbb{I}-Z^{\mathrm{I}})_i (X_i^{\mathrm{III}} X_{i+1}^{\mathrm{II}} + X_i^{\mathrm{II}} X_{i+1}^{\mathrm{III}})] - \frac{1}{2}\sum_i \boldsymbol{[\mathbb{I}+Z^{\mathrm{I}}]_i}$ 
SPT	$\boldsymbol{H_{(\mathbb{Z}_2^a \times \mathbb{Z}_2^b)^-} \simeq -\frac{1}{2}\sum_i \frac{1}{2}(\mathbb{I}+Z^{\mathrm{I}})_i [\boldsymbol{X_i^{\mathrm{II}}(X^{\mathrm{II}}Z^{\mathrm{III}})_{i+1} + (Z^{\mathrm{II}}X^{\mathrm{III}})_i X_{i+1}^{\mathrm{III}}}] - \frac{1}{2}\sum_i \boldsymbol{[\mathbb{I}+Z^{\mathrm{I}}]_i}}$ $-\frac{1}{2}\sum_i \frac{1}{2}(\mathbb{I}-Z^{\mathrm{I}})_i (X_i^{\mathrm{III}} X_{i+1}^{\mathrm{II}} + (Z^{\mathrm{III}}X^{\mathrm{II}})_i X_{i+1}^{\mathrm{III}})$, $\lvert \mathrm{GS}\rangle \circlearrowleft$
$\mathbb{Z}_2$ SSB	$H_{\mathbb{Z}_2^c} = -\frac{1}{2}\sum_i \mathbb{I}_i\mathbb{I}_{i+1} - \frac{1}{2}\sum_i X_i^{\mathrm{I}} [\frac{1}{2}(\mathbb{I}+Z^{\mathrm{II}}Z^{\mathrm{III}})X^{\mathrm{I}} + \frac{1}{2}(\mathbb{I}-Z^{\mathrm{II}}Z^{\mathrm{III}})X^{\mathrm{I}}X^{\mathrm{II}}X^{\mathrm{III}}]_{i+1} - \frac{1}{4}\sum_i [(\mathbb{I}+Z^{\mathrm{II}})(\mathbb{I}+Z^{\mathrm{III}})]_i$ 
$\mathbb{Z}_2 \times \mathbb{Z}_2$ SSB	$H_{(\mathbb{Z}_2^c \times \mathbb{Z}_2^{ab})^+} \simeq -\frac{1}{2}\sum_i X_i^{\mathrm{I}} [\frac{1}{2}(\mathbb{I}+Z^{\mathrm{II}}Z^{\mathrm{III}})X^{\mathrm{I}} + \frac{1}{2}(\mathbb{I}-Z^{\mathrm{II}}Z^{\mathrm{III}})X^{\mathrm{I}}X^{\mathrm{II}}X^{\mathrm{III}}]_{i+1}$ $-\frac{1}{2}\sum_i [(X^{\mathrm{II}}X^{\mathrm{III}})_i (X^{\mathrm{II}}X^{\mathrm{III}})_{i+1}] - \frac{1}{2}\sum_i [\mathbb{I} + (Z^{\mathrm{II}}Z^{\mathrm{III}})]_i$ 
SPT	$H_{(\mathbb{Z}_2^c \times \mathbb{Z}_2^{ab})^-} \simeq -\frac{1}{8}\sum_i X_i^{\mathrm{I}} [(\mathbb{I}+Z^{\mathrm{II}}Z^{\mathrm{III}})X^{\mathrm{I}} + (\mathbb{I}-Z^{\mathrm{II}}Z^{\mathrm{III}})X^{\mathrm{I}}X^{\mathrm{II}}X^{\mathrm{III}}]_{i+1}$ $[\mathbb{I}+Z^{\mathrm{II}}+Z^{\mathrm{III}}-Z^{\mathrm{II}}Z^{\mathrm{III}}]_{i+1} - \frac{1}{2}\sum_i [(Z^{\mathrm{I}}X^{\mathrm{II}}X^{\mathrm{III}})_i (X^{\mathrm{II}}X^{\mathrm{III}})_{i+1}]$ $-\frac{1}{2}\sum_i [\mathbb{I} + (Z^{\mathrm{II}}Z^{\mathrm{III}})]_i$, $\lvert \mathrm{GS}\rangle \circlearrowleft$
$\mathbb{Z}_2$ SSB	$H_{(D_8)^-} = -\frac{1}{8}\sum_i [(\mathbb{I}+Z^{\mathrm{I}})X^{\mathrm{II}} + (\mathbb{I}-Z^{\mathrm{I}})X^{\mathrm{III}}]_i X_{i+1}^{\mathrm{II}} [\mathbb{I}-Z^{\mathrm{I}}+Z^{\mathrm{III}}+Z^{\mathrm{I}}Z^{\mathrm{III}}]_{i+1} - \sum_i \mathbb{I}_i$ $-\frac{1}{8}\sum_i [\mathbb{I}+Z^{\mathrm{II}}+Z^{\mathrm{III}}-Z^{\mathrm{II}}Z^{\mathrm{III}}]_i X_i^{\mathrm{I}} [(\mathbb{I}+Z^{\mathrm{II}}Z^{\mathrm{III}})X^{\mathrm{I}} + (\mathbb{I}-Z^{\mathrm{II}}Z^{\mathrm{III}})X^{\mathrm{I}}X^{\mathrm{II}}X^{\mathrm{III}}]_{i+1}$ 
$\mathbb{Z}_2 \times \mathbb{Z}_2$ SSB	$H_{\mathbb{Z}_4^{ca}} \simeq -\frac{1}{4}\sum_i [(\mathbb{I}+Z^{\mathrm{I}})X^{\mathrm{I}}X^{\mathrm{III}} + (\mathbb{I}-Z^{\mathrm{I}})X^{\mathrm{I}}X^{\mathrm{II}}]_i [X^{\mathrm{I}}X^{\mathrm{III}}(\mathrm{Swap})^{\mathrm{II,III}}]_{i+1}$ $-\frac{1}{4}\sum_i [(\mathbb{I}+Z^{\mathrm{I}})X^{\mathrm{I}}X^{\mathrm{II}} + (\mathbb{I}-Z^{\mathrm{I}})X^{\mathrm{I}}X^{\mathrm{III}}]_i [X^{\mathrm{I}}X^{\mathrm{II}}(\mathrm{Swap})^{\mathrm{II,III}}]_{i+1} - \frac{1}{2}\sum_i [\mathbb{I}+Z^{\mathrm{I}}Z^{\mathrm{II}}Z^{\mathrm{III}}]_i$ 
$\mathsf{Rep}(D_8)$ SSB	$H_{(D_8)^+} \simeq -\frac{1}{4}\sum_i [(\mathbb{I}+Z^{\mathrm{I}})X^{\mathrm{II}} + (\mathbb{I}-Z^{\mathrm{I}})X^{\mathrm{III}}]_i X_{i+1}^{\mathrm{II}} - \sum_i \mathbb{I}_i$ $-\frac{1}{4}\sum_i X_i^{\mathrm{I}} [(\mathbb{I}+Z^{\mathrm{II}}Z^{\mathrm{III}})X^{\mathrm{I}} + (\mathbb{I}-Z^{\mathrm{II}}Z^{\mathrm{III}})X^{\mathrm{I}}X^{\mathrm{II}}X^{\mathrm{III}}]_{i+1}$ 